SSD-TR-92-07

AEROSPACE REPORT NO.
TR-0091(6940-05)-2

AD-A252 394

The Energetic Radiation Environment in a Highly Elliptical (Molniya) Orbit

Prepared by

J. B. BLAKE
Space and Environment Technology Center
Technology Operations

15 May 1992

Prepared for

SPACE SYSTEMS DIVISION
AIR FORCE SYSTEMS COMMAND
Los Angeles Air Force Base
P. O. Box 92960
Los Angeles, CA 90009-2960

Engineering and Technology Group

92-17494

THE AEROSPACE CORPORATION
El Segundo, California

92

UNCLASSIFIED
SECURITY CLASSIFICATION OF THIS PAGE

REPORT DOCUMENTATION PAGE

1a. REPORT SECURITY CLASSIFICATION Unclassified	1b. RESTRICTIVE MARKINGS
2a. SECURITY CLASSIFICATION AUTHORITY	3. DISTRIBUTION/AVAILABILITY OF REPORT Approved for public release; distribution unlimited
2b. DECLASSIFICATION/DOWNGRADING SCHEDULE	
4. PERFORMING ORGANIZATION REPORT NUMBER(S) TR-0091(6940-05)-2	5. MONITORING ORGANIZATION REPORT NUMBER(S) SSD-TR-92-07
6a. NAME OF PERFORMING ORGANIZATION The Aerospace Corporation Technology Operations 6b. OFFICE SYMBOL (If applicable)	7a. NAME OF MONITORING ORGANIZATION Space Systems Division
6c. ADDRESS (City, State, and ZIP Code) El Segundo, CA 90245-4691	7b. ADDRESS (City, State, and ZIP Code) Los Angeles Air Force Base Los Angeles, CA 90009-2960
8a. NAME OF FUNDING/SPONSORING ORGANIZATION 8b. OFFICE SYMBOL (If applicable)	9. PROCUREMENT INSTRUMENT IDENTIFICATION NUMBER F04701-88-C-0089
8c. ADDRESS (City, State, and ZIP Code)	10. SOURCE OF FUNDING NUMBERS PROGRAM ELEMENT NO. / PROJECT NO. / TASK NO. / WORK UNIT ACCESSION NO.

11. TITLE *(Include Security Classification)*

The Energetic Radiation Environment in a Highly Elliptical (Molniya) Orbit

12. PERSONAL AUTHOR(S)
Blake, J. Bernard

13a. TYPE OF REPORT	13b. TIME COVERED	14. DATE OF REPORT (Year, Month, Day)	15. PAGE COUNT
	FROM ______ TO ______	15 May 1992	9

16. SUPPLEMENTARY NOTATION

17. COSATI CODES

FIELD	GROUP	SUB-GROUP

18. SUBJECT TERMS *(Continue on reverse if necessary and identify by block number)*
Molniya Orbit
NASA AE-8 Model
NASA AP-8 Model
Space Radiation Environment

19. ABSTRACT *(Continue on reverse if necessary and identify by block number)*

Measurements have been made of the dose received by silicon components under 100 mils of aluminum aboard satellites in a Molniya orbit. Nearly continuous data are presented for the time period from August 1983 until March 1990. It is concluded that the observations are consonant with the predictions of the NASA AP-8 model but not with those of the AE-8 model.

20. DISTRIBUTION/AVAILABILITY OF ABSTRACT
[X] UNCLASSIFIED/UNLIMITED [ ] SAME AS RPT [ ] DTIC USERS

21. ABSTRACT SECURITY CLASSIFICATION
Unclassified

22a. NAME OF RESPONSIBLE INDIVIDUAL	22b. TELEPHONE (Include Area Code)	22c. OFFICE SYMBOL

DD FORM 1473, 84 MAR — 83 APR edition may be used until exhausted. All other editions are obsolete.

SECURITY CLASSIFICATION OF THIS PAGE
UNCLASSIFIED

CONTENTS

FIGURES

TABLES

THE ENERGETIC RADIATION ENVIRONMENT IN A HIGHLY ELLIPTICAL (MOLNIYA) ORBIT

J. B. Blake
Space and Environment Technology Center
The Aerospace Corporation
Los Angeles, CA USA

I. INTRODUCTION

A simple dosimeter has been flown aboard two satellites in Molniya orbits which measures the radiation dose under 0.69 gm/cm^2 ($\approx$ 100 mils) of aluminum. For convenience and historical reasons the measurements are labeled as PLO3 and PLO4. The measurements have been made almost continuously since August 1983.

A Molniya orbit has an inclination of 63° and a period of just under 12 hours. The inclination and perigee are selected such that the argument of perigee does not change with time, and the satellite remains above the same two regions of the Earth every day. Perigee is made as low as possible in order to maximize the dwell period around apogee.

A satellite in a Molniya orbit encounters a variety of magnetospheric environments, including the inner zone with intense fluxes of energetic protons resulting from the CRAND (cosmic ray albedo neutron decay) process, the outer zone with high, time-variable fluxes of energetic electrons, the Southern auroral zone, the high-latitude plasma sheet, the magnetosheath, and the interplanetary medium. From the point of view of electronic systems, it is the energetic particles which are of primary concern because of total dose and single event upset considerations.

II. THE INSTRUMENTS

The two dosimeters were designed, fabricated, and tested by the Space and Environment Technology Center of The Aerospace Corporation. Each dosimeter uses a single silicon surface-barrier detector; its electronic system measures the ionization in each silicon disc caused by the ambient radiation. The geometrical configuration of the sensor is that of a semi-infinite slab, with only 1/2 of the 2π solid angle exposed to the ambient environment. The other π solid angle, as well as the rear 2π solid angle of the slab, is very heavily shielded. Details of the instrumentation may be found in Blake and Cox (Ref. 1).

Data are acquired only around apogee, where the dose rate is nil except in the case of a solar particle event. Thus, these experiments provide only a measurement of the dose integrated over an orbit.

III. RESULTS

Figure 1 is a plot of the dosimeter measurements between August 1983 and February 1989. Several characteristics of the data are immediately apparent:

1. The dose per day is highly variable.
2. The fluctuations in dose are superimposed upon a baseline dose which varies slowly with time, both increasing and decreasing.
3. Upon occasion, abrupt enhancements in dose appear to be periodic, for example, around November 1984.
4. The "baseline" doses in the two dosimeters in general are not the same although they exhibit similar periodicities and magnitudes.

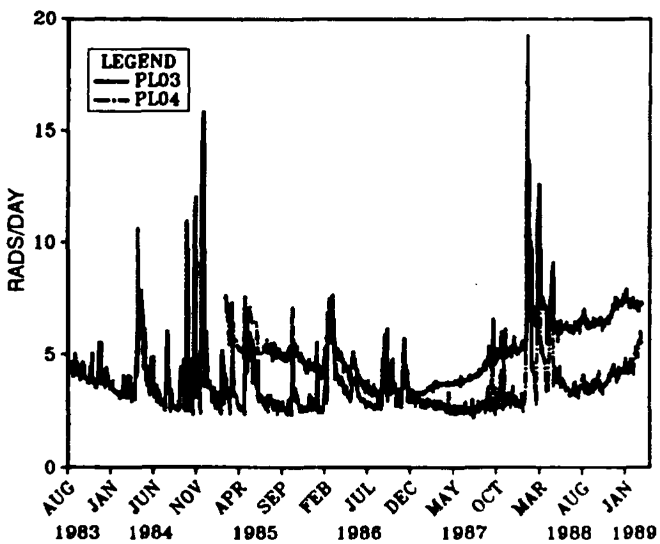

Figure 1. A plot of the daily dose measurements made between August 1983 and February 1989.

Figure 2 shows how the perigee altitude varied with time. This figure, when compared with Figure 1, shows that the perigee altitude is a major factor in determining the baseline dose. The baseline dose can be seen to be inversely dependent upon the perigee altitude. Note also the comforting fact that when the satellites have the same perigee altitude, the measured doses are essentially equal.

This issue can be pursued further. Figure 3 is a plot of the dose measured from both sensors during August 1987, divided into Atlantic and Pacific orbits. This period

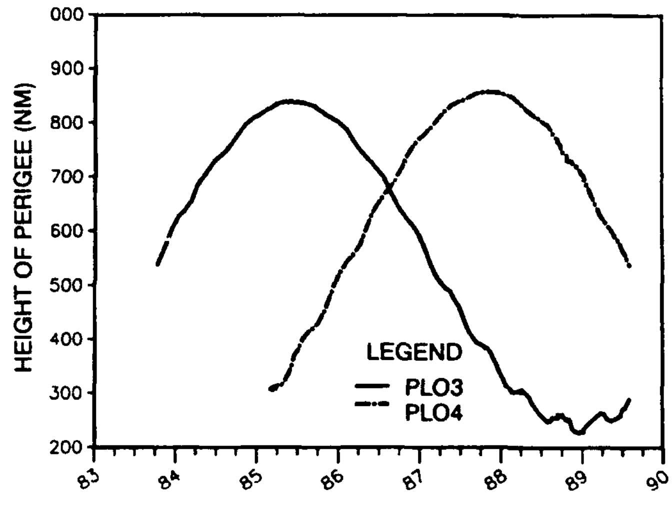

Figure 2. A plot of the time dependence of perigee altitudes as a function of time.

was selected because it was a relatively lengthy quiet period. (The definition of Atlantic and Pacific orbits is based upon the longitude of perigee of the host satellite. Both satellites are stationed at the same longitudes but pass perigee at different times in a day.) A dramatic difference can be seen in the dose per orbit, depending upon both perigee altitude and perigee longitude.

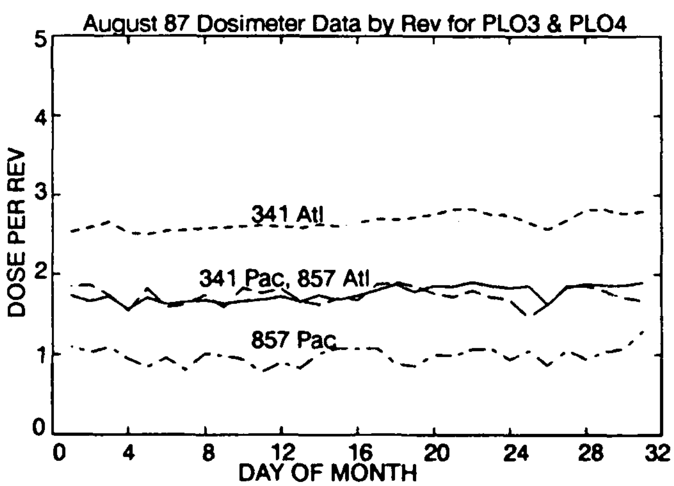

Figure 3. The measured daily dose is separated into Atlantic and Pacific (perigee) orbits.

The underlying physics can be seen by plotting the trajectories of the satellites in **B,L** space (Figure 4). Clearly, when perigee is lower, the satellite moves deeper into the region occupied by the inner-zone energetic protons and, because of the effect of the South Atlantic Magnetic Anomaly, higher fluxes are encountered on the Atlantic orbit.

An important conclusion may be drawn from these findings. *The baseline dose is largely due to the energetic protons; the energetic electrons make little contribution to the baseline dose.* As pointed out in Blake and Cox (Ref. 1), this finding is in conflict with the predictions for a Molniya orbit given by the AE-8 and AP-8 models, and led them to conclude that the AE-8 model substantially overpredicts the dose received in a Molniya orbit under the dosimeter shield of 100 mils of aluminum. This point is discussed further below.

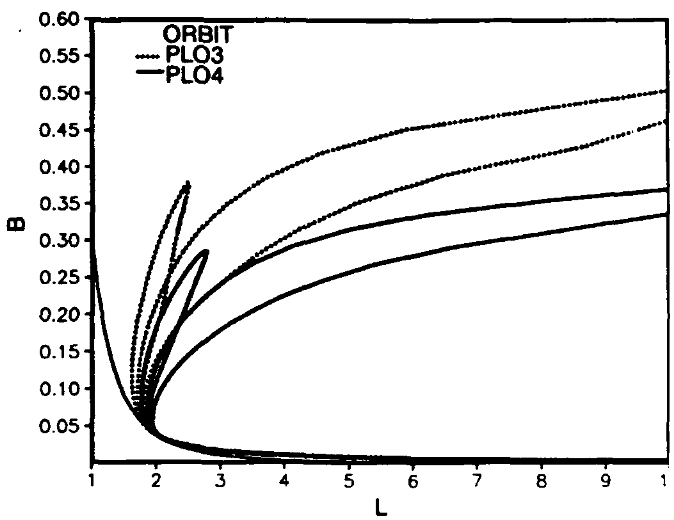

Figure 4. This figure shows a representative case of the trajectories of the two spacecraft in **B,L** space during August 1987.

The fluctuations in dose seen above the baseline are not surprising considering the well-known, highly variable population of energetic outer-zone electrons. Although not shown here, these enhancements in dose are well correlated with geomagnetic activity. The periodic large spikes reoccur at the synodic period of the sun. It was discovered by Paulikas and Blake (Ref. 2) that such enhancements were due to the presence of high-speed solar wind streams interacting with the magnetosphere of the Earth(in a way not yet well understood). The reoccurrence results when a high-speed solar-wind stream emitted from a coronal hole is stable over a period of a few months — every time the stream sweeps over the Earth the energetic electron population markedly increases a few days later. Such observations have been discussed further by Baker et al. (Ref. 3).

One of the largest magnetic storms on record occurred in mid-March 1989. This storm caused a major change in the baseline dose. Figure 5 is a plot of the data between May 1987 and May 1989. There was a relatively rapid decrease in dose in mid-March, followed by a gradual decay continuing at least until July. As can be seen by examining the previous time histories of the baseline dose and the height of perigee (Figures 1 and 2), a fundamental change has occurred. The magnetic storm of March 1989 caused a redistribution and/or loss of the CRAND protons in at least the outer regions (L > ~1.6) of the inner zone. McIlwain (Ref. 4) has reported an abrupt redistribution of energetic protons at the time of a large storm at somewhat higher L values. The present measurements do not allow us to determine what occurred in any detail.

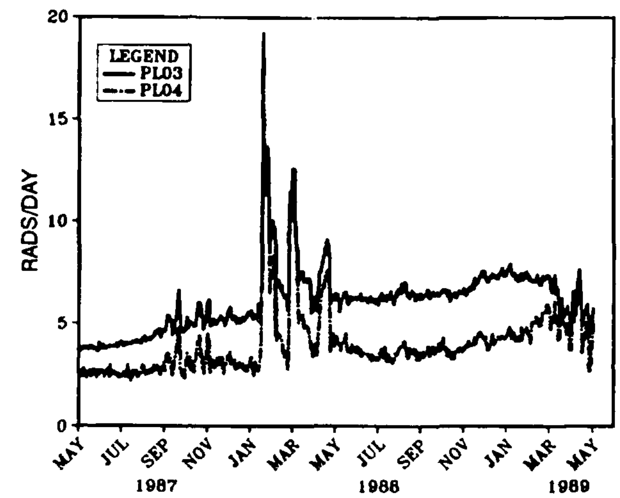

Figure 5. A plot of the dosimeter data acquired between May 1987 and May 1989.

Unfortunately, the further evolution of the dose with time became confused by the series of large solar particle events in the August-November time period. Figure 6 is a plot of the measured dose between March 1989 and April 1990. The presence of the solar particles can be seen clearly.

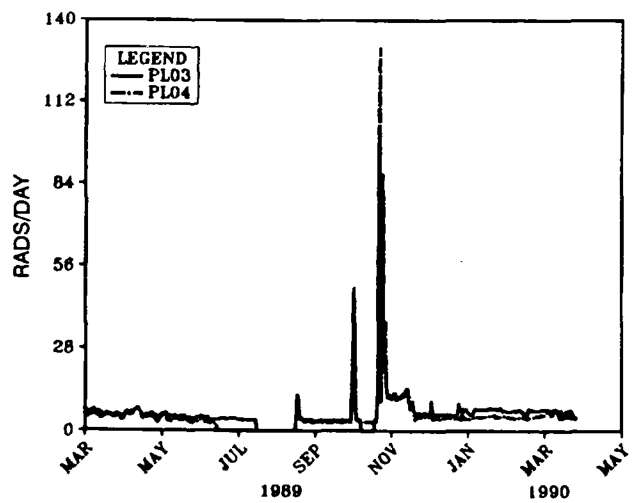

Figure 6. A plot of the dosimeter data acquired between March 1989 and April 1990.

The data in September 1989 suggest that the decay of the baseline dose had ended by that time. The data from December 1989 onwards indicate that the baseline dose had increased by December but appeared to change little afterwards. It is possible that the increased baseline dose has been brought about by the SPAND (solar proton albedo neutron decay) process, and does not indicate a recovery of the CRAND protons from the effects of the March 1989 storm. The limited nature of the dosimeter measurements can only tantalize us but not supply definitive answers to these questions; they were intended only to supply engineering information.

The solar particles increased the daily dose up to a factor of almost 30. Although this is a dramatic increase, over mission lifetimes measured in years, the solar particle dose is negligible.

IV. DISCUSSION

The dosimeter aboard the satellite launched in August 1983 measured an average dose of 4.52 rads/day over a period of 1996 days; the dosimeter launched in February 1985 measured an average dose of 4.20 rads over a period of 1447 days. The difference is not surprising considering that the satellites were launched into orbits with a different perigee phase (*cf.* Figure 2). The expected dose was calculated using the NASA AE-8 and AP-8 environmental models to determine the particle fluence impinging upon the dosimeter and using the Shieldose program to convert the fluences to a depth-dose profile. Because only 1/2 of the semi-infinite slab geometry of the dosimeter was exposed to the space environment, the measured doses must be multiplied by 2 when making a comparison with the model calculations.

Table 1 gives the predicted dose for solar minimum, Table 2, for solar maximum.

Table 1. Solar Minimum Dose — 100 Mils of Aluminum

Perigee Altitude and Location	e-Dose	Brems.-Dose	p-Dose	Total Dose
341 nm-Atlantic	5.60 rads	0.12	4.12	9.84
341 nm-Pacific	8.98	0.16	3.30	12.4
857 nm-Atlantic	5.62	0.12	3.37	9.11
857 nm-Pacific	11.4	0.19	1.66	13.2

Table 2. Solar Maximum Dose — 100 Mils of Aluminum

Perigee Altitude and Location	e-Dose	Brems.-Dose	p-Dose	Total Dose
341 nm-Atlantic	9.86 rads	0.31	4.11	14.3
341 nm-Pacific	15.5	0.38	3.29	19.2
857 nm-Atlantic	10.2	0.31	3.37	13.9
857 nm-Pacific	19.2	0.39	1.66	22.0

A comparison of the two tables shows that the predicted proton doses are independent of position in the solar cycle but that the predicted electron doses are substantially larger at solar maximum. If one compares the data in Figure 3 with the total doses given in Table 1 and Table 2, one can see that there are very large discrepancies in magnitude, altitude, and longitude dependence. There simply is no fit between prediction and measurement!

However, if one compares the data in Figure 3 with only the proton dose in Table 1 and Table 2, a good fit can be seen. The 341 nm-Atlantic rev shows the largest dose, the 341 nm-Pacific and the 857 nm-Atlantic revs are essentially identical, while the 857 nm-Pacific rev shows the smallest dose. The measured doses are somewhat higher, perhaps 30% (remember the factor of 2 required to compare measurement with prediction discussed previously). This is compelling evidence that the dose received by a satellite in a Molniya orbit is dominated by the inner-zone protons during quiet times.

Tables 1 and 2 show that the predicted electron doses are substantially higher at solar maximum. In Figure 7, the daily dose is plotted for just the first satellite launched for greater clarity. If one mentally subtracts the baseline dose due to protons, it can be seen that the greater electron dose rates were not observed around solar maximum but rather in the 1984 and 1985 time period, during the approach to solar minimum.

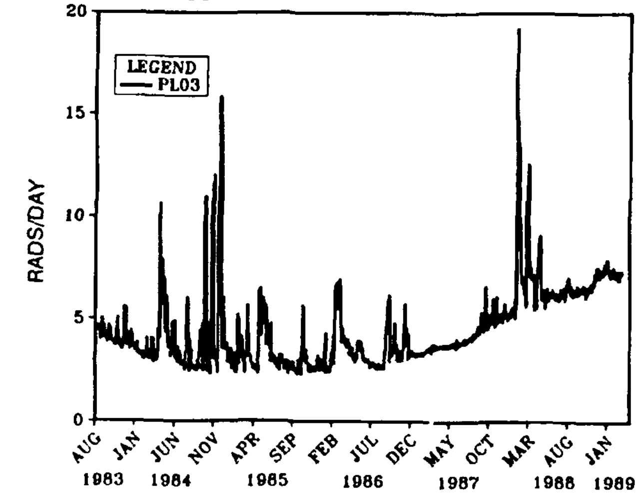

Figure 7. A plot of the dosimeter data from PLO3 which illustrates the time periods when the daily dose was enhanced.

V. CONCLUSIONS

The dosimeter measurements discussed in this report indicate that the AP-8 models lead to dose predictions consonant with the observations but that the AE-8 models do not. It must be noted this result is for a single shielding thickness, 100 mils of Al, and for a single orbit, a Molniya orbit.

One could argue that there might be uncertainties in the absolute calibration of the dosimeters which might lead to discrepancies between observations and predictions. However, the temporal, spatial, and altitude dependence of the observed dose is in disagreement with the electron predictions, and these discrepancies are not eliminated by postulating an uncertainty in the dosimeter sensitivity.

REFERENCES

[1] J. B. Blake and J. E. Cox 1989, The Radiation in a Molniya-Type Orbit, in *High Energy Radiation Background in Space*, Eds. A. C. Rester, Jr. and J. I. Trombka, AIP Conference Proceedings 186, American Institute of Physics, New York, 297.

[2] G. A. Paulikas and J. B. Blake 1979, in *Quantitative Modeling of Magnetospheric Processes*, Ed. W. P. Olsen, Geophysical Monograph Series 21, American Geophysical Union, Washington, 180.

[3] D. N. Baker, J. B. Blake, R. W. Klebesadel, and P. R. Higbie 1986, *Journal Geophysical Research*, 89, 4265.

[4] C. E. McIlwain 1965, Redistribution of Trapped Protons during a Magnetic Storm, *Space Research*, 5, 374.

TECHNOLOGY OPERATIONS

The Aerospace Corporation functions as an "architect-engineer" for national security programs, specializing in advanced military space systems. The Corporation's Technology Operations supports the effective and timely development and operation of national security systems through scientific research and the application of advanced technology. Vital to the success of the Corporation is the technical staff's wide-ranging expertise and its ability to stay abreast of new technological developments and program support issues associated with rapidly evolving space systems. Contributing capabilities are provided by these individual Technology Centers:

Electronics Technology Center: Microelectronics, solid-state device physics, VLSI reliability, compound semiconductors, radiation hardening, data storage technologies, infrared detector devices and testing; electro-optics, quantum electronics, solid-state lasers, optical propagation and communications; cw and pulsed chemical laser development, optical resonators, beam control, atmospheric propagation, and laser effects and countermeasures; atomic frequency standards, applied laser spectroscopy, laser chemistry, laser optoelectronics, phase conjugation and coherent imaging, solar cell physics, battery electrochemistry, battery testing and evaluation.

Mechanics and Materials Technology Center: Evaluation and characterization of new materials: metals, alloys, ceramics, polymers and their composites, and new forms of carbon; development and analysis of thin films and deposition techniques; nondestructive evaluation, component failure analysis and reliability; fracture mechanics and stress corrosion; development and evaluation of hardened components; analysis and evaluation of materials at cryogenic and elevated temperatures; launch vehicle and reentry fluid mechanics, heat transfer and flight dynamics; chemical and electric propulsion; spacecraft structural mechanics, spacecraft survivability and vulnerability assessment; contamination, thermal and structural control; high temperature thermomechanics, gas kinetics and radiation; lubrication and surface phenomena.

Space and Environment Technology Center: Magnetospheric, auroral and cosmic ray physics, wave-particle interactions, magnetospheric plasma waves; atmospheric and ionospheric physics, density and composition of the upper atmosphere, remote sensing using atmospheric radiation; solar physics, infrared astronomy, infrared signature analysis; effects of solar activity, magnetic storms and nuclear explosions on the earth's atmosphere, ionosphere and magnetosphere; effects of electromagnetic and particulate radiations on space systems; space instrumentation; propellant chemistry, chemical dynamics, environmental chemistry, trace detection; atmospheric chemical reactions, atmospheric optics, light scattering, state-specific chemical reactions and radiative signatures of missile plumes, and sensor out-of-field-of-view rejection.